IEEE Access
Multidisciplinary ⋮ Rapid Review ⋮ Open Access Journal

Received August 31, 2021, accepted September 3, 2021, date of publication September 7, 2021, date of current version September 16, 2021.

Digital Object Identifier 10.1109/ACCESS.2021.3111021

Automatic Segmentation and Detection System for Varicocele in Supine Position

OMAR ALZOUBI [1], MOHAMMAD ABU AWAD [1], AND AYMAN M. ABDALLA [2]
[1]Department of Computer Science, Jordan University of Science and Technology, Irbid 22110, Jordan
[2]Department of Computer Science, Al-Zaytoonah University of Jordan, Amman 11733, Jordan

Corresponding author: Omar Alzoubi (oaalzoubi@just.edu.jo)

ABSTRACT Image analysis is an important technique that can help specialists localize, detect, and segment objects in different types of medical images such as MRI, CTs, and ultrasounds (US). In this research, we use US images to identify and segment the enlarged veins in the pampiniform venous plexus, which is called varicocele. The proposed method aims to determine whether a potential patient is affected or not. This method was evaluated using 90 US images that were taken of the left testicles of 90 patients in the Supine position. This system analyzes US images in three stages which are; preprocessing, processing, and edge detection. The Region Of Interest (ROI) of the pampiniform plexus area was extracted using Otsu segmentation with different parameters (0.1, 0.2, 0.17) and different color modes (Grayscale, YCbCr, RGB). In the processing stage, different denoising filters were used. Eventually, in the edge detection stage, four edge detectors were applied which are Canny, Soble, Prewitt, and Roberts. Results showed that the best accuracy in detecting varicocele was 78% when the YCbCr color mode yellow (y) channel was used with 0.1 Otsu segmentation and the Canny edge detector. The system also showed a Sensitivity of 91%, as the test was able to detect 91% of the people with Varicocele, and the Specificity value was 39%.

INDEX TERMS Varicocele, Otsu segmentation, canny, ultrasound image, color mode.

I. INTRODUCTION

Computer vision and image analysis technology operate in various engineering fields such as object detection [1], [2], 3D image reconstruction [3], and medical image analysis [4]. Ultrasound (US) is a widely used medical imaging technique. It has advantages and characteristics that make it accessible to all patients. It is safe, inexpensive, and fast. The need for segmentation of US images appeared in many medical examinations. For example, it is used in obstetrics for obtaining fetus measurements like femur length and head circumference, and in cardiovascular applications [5]. It could also be used in vessel detection applications of various types of veins such as intercostal veins and pampiniform plexus veins.

Varicocele is an abnormal tortuosity or dilatation of the pampiniform venous plexus. It usually occurs in 10-15% of men and adolescent males. From a clinical view, varicocele is expressed by the presence of a palpable, little scrotal mass and is rarely accompanied by moderate pain. Also, varicocele may be associated with infertility since there is a relationship between male infertility, sperm alteration, and varicocele. It usually occurs in 30%-40% of patients infected with varicocele [6]. Varicocele has no symptoms in general but it may cause scrotal pain and discomfort. This pain occurs when the patient makes a strong effort or sits for a long time or stands in the wrong posture. The pain intensity is comparable to a toothache. This pain does not spread to the rest of the body [7] and the patient feels comfortable after lying down so that the pain is gradually relieved. However, varicocele pain can hardly be sensed by the patient till the scrotal wall becomes thick and contracted.

Color Doppler Ultrasound (CDUS) is a technique that can be used to examine varicose veins [8] and take a picture of the testicles and surrounding tissues. Ultrasound imaging is used to identify abnormalities in the testes, epididymis, and scrotum. In this paper, we used 2D ultrasound images for the diagnosis of varicocele. The diagnosis of varicocele is performed in three positions: supine, valsalva, and standing [9]. Most experiments are executed in the supine position since the majority of specialists depend on it for diagnosis. The supine or dorsal position is the most common position used in the examination room. Typically, the head is rested on a foam

The associate editor coordinating the review of this manuscript and approving it for publication was Orazio Gambino.

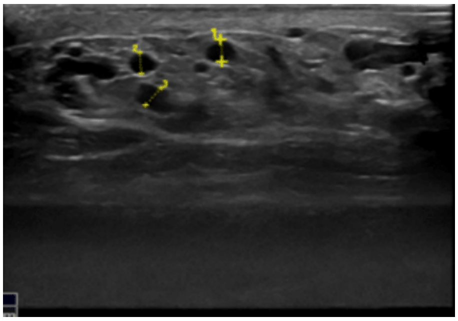

FIGURE 1. Varicocele in supine position.

pillow, keeping the neck in a neutral position. The patient's arms are tucked at his sides. Fig. 1 shows an ultrasound image of a patient who has varicocele taken in a supine position [10].

Despite extensive prior studies in veins detection, there is little research done on detecting varicocele from 2D US images. The purpose of this paper is to determine if a probable patient is affected by varicocele through detecting dilated veins in the US images by utilizing image processing techniques. Choosing automatic detection of varicocele is driven by many motives. First, ultrasound images are inexpensive and the automatic detection of varicocele can reduce dependence on experienced radiologists especially in remote areas. Second, most of the previous work focused on detecting and identifying vessels in different organs, like cardiovascular and retinal vessels where this study focuses on veins in the testicle area that affect men's fertility. The novel method of this paper presents the following main contributions:

- Detecting dilated veins in pampinform plexus venosus in ultrasound images.
- Detecting two structures of the veins: cross-section structure and tube structure.
- Detecting many dilated veins of different shapes in the same image, which is a valuable contribution.

Our results showed that the accuracy of determining if a patient is affected by varicocele was 78%. This was obtained by utilizing the YCbCr color mode yellow (y) channel with 0.1 Otsu segmentation and the Canny edge detector.

The remainder of this paper is organized as follows; Sec II provides a review of the literature. Sec III illustrates the methods and data collection. Sec IV presents our results and discusses the main findings. Finally, Sec V concludes this research and provides plans for future work.

II. RELATED WORK

Image segmentation algorithms of medical images of anatomical form have become more important over time for automating a wide set of radiological tasks. They play a vital role in numerous biomedical imaging applications like diagnosis, localization of pathology, and treatment planning [11]. Image segmentation is defined as "the partitioning of an image into non-overlapping, constituent regions that are homogeneous concerned with some characteristic such as intensity or texture" [12]. The methods that use image segmentation include Markov random field (MRF) models, region growing, thresholding, classifiers, clustering, artificial neural networks, deformable models, and atlas-guided approaches. This section only reviews those methods closely related to this paper [13].

In a preliminary study, image processing techniques were applied to enhance the 2D ultrasound image to help the diagnosis [14]. The images used were of normal testicles, testicles with varicocele, and testicles with severe varicocele. The algorithms they used were the median filter and Sobel operator. A median filter was computed in three steps; arranging the neighboring pixels into numerical order, finding the middle pixel value, and replacing all the neighboring pixels value with the middle pixel value. The image was cropped so that only the testicle region would be examined. Finally, the edge detection operation was performed using a Sobel operator. Results showed that the Sobel technique enhanced the varicocele region, especially the dilated veins. They used MSE and PSNR to evaluate the performance.

A method was proposed for segmenting and tracking the internal jugular vein (IJV) and it employed the optical flow as a vector field that connects each frame to the next frame using the Lucas-Kanade (LK), Horn-Schunck (HS), and Farneback (FB) algorithms [15]. First, the LK algorithm partitioned the image into smaller blocks and assumed that the pixel shift is constant. In the next step, the FB algorithm was used to calculate the cost of the displacement vector assuming that the flow vector field is smooth. Finally, the HS algorithm approximated the neighborhood of the pixel of each frame with a quadratic polynomial. Results showed that the algorithm provided a good level of agreement with manual segmentation.

An algorithm was developed for the automatic detection of microaneurysms by using thresholding and mathematical morphology techniques [16]. These techniques were used for detecting MAs from the RGB fundus image. Preprocessing was done for resizing the input image and extracting the green channel. The exudates were removed by using the thresholding technique, which is Canny edge detection. Then, the median filtering technique was used to reduce noise. Morphological methods were used for eliminating the Optic Disc (OD) and blood vessels. The data set they used was DIARETDB1, which contains 89 RGB fundus images. These images had various infected components like exudates and hemorrhages. Note that this previous work used only RGB images. In contrast, our research used three color modes; RGB, Grayscale, and YCbCr.

A system was proposed for automatically identifying, segmenting, and tracking the cross-section of the internal jugular vein (IJV) and the common carotid artery (CCA) by using an ultrasound image feed during a central venous catheter (CVC) placement procedure [17]. Star algorithm was used for the segmentation, implementation, and tracking of the blood vessel. Using this algorithm, the locations of the IJV and the CCA were identified in two important steps. First, specifying the initial starting point at the beginning of the trace. Second, checking the fragmentation results for every subsequent window. Ellipse parameters were used to investigate the blood vessel classification to assess the physical characteristics of the blood vessel cross-section. A support vector machine (SVM) was used to implement the cascading classifier in two steps. First, classifying blood vessel and non-vessel structures and, second, classifying the IJV and CCA. Five features were used for measuring the accuracy using F-measure. Results showed that the system using a cascading manner may be able to identify the IJV and CCA cross-section in ultrasound image frames with high accuracy in real-time.

Detecting the Morphological changes of retinal vessels like arteriovenous (AV) nicking was investigated by Kang *et al.* [18]. An automatic method was used and it included crossover point detection and AV-nicking identification. First, the image was prepared by using multiscale line detection and vascular boundary information. Then crossover points from vessel segmentation and centerline extraction were applied, and vessels in the crossing area were classified into arteries and veins.

A method for processing carotid arteries using ultrasonic images was proposed by Licev *et al.* [19]. The Hough transform (HT) was used for artery detection, and an active contour based on level set methods was modified and used for object segmentation. A CLAHE (Contrast Limited Adaptive Histogram Enhancing) method was used for preprocessing the image. A median filter was used for reducing the transfer function slope and for removing the speckle noise. The classical Sobel filter was used for edge detection and iterative adaptive thresholding. Finally, a local Gaussian distribution fitting energy was employed for describing the detailed arterial shape. The method achieved a reliability rate of 79.1% for artery detection.

An algorithm was proposed by Ghadiri *et al.* for detecting vessels in retinal analysis for extracting information including changes in blood vessels [20]. This method was based on fuzzy inference and edge detection. Linear structures were used where the image was divided into overlapping windows. A Sobel operator was then used for extracting edges along with the predetermined direction. A genetic algorithm was then applied and it helped in the vessel validation process. Finally, vessel shapes were reconstructed via morphological algorithms. This algorithm achieved performance higher than some other detection algorithms.

III. DATA AND METHODS

In this paper, we present an algorithm designed for detecting varicocele from US images and it employs image segmentation. Segmentation is an important technique applied in different fields of image processing and it is usually used for detecting objects of interest in a medical image. In the biomedical field, segmentation is normally applied for post-processing medical images, especially ultrasound images. Generally, segmentation supports the automatic detection and exploration of diseases in medical images [21].

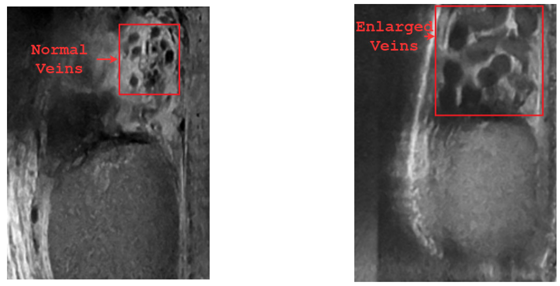

(a) Ultrasound with normal Veins (b) Ultrasound with enlarged Veins (varicocele)

FIGURE 2. **Ultrasound of a testicle showing normal and enlarged veins (varicocele).**

A. DATA COLLECTION

Ninety US images of normal and abnormal (varicocele) cases were collected from the Department of Radiology at a local hospital in Amman, Jordan. The US examinations were performed on 90 men, aged 13-63, from April 2018 to September 2018. The US examination of the pampiniform plexus venous (PPV) for the left test was performed by two specialists. The images were extracted as DICOM images and then converted into PNG format. The US image can be developed at a high frequency for exploring superficial tissues, so US imaging can be the best choice for discovering varicocele. Figure 2 shows normal and abnormal images in varicocele disease detection. Figure 2-(a) shows a normal image with veins surrounding the testicle in non-dilated form, while Fig. 2-(b) shows an abnormal image with dilated veins that appear clearly in the testicle area.

B. SYSTEM DESCRIPTION

Our novel system has been designed to identify the region of interest (ROI) from a US image and then detect dilated veins in this region by employing different enhancement, denoising, and edge detection algorithms. A flowchart of this proposed system is illustrated in Fig. 3. The system consists of three stages; preprocessing, processing, and edge detection where each stage consists of multiple steps. The preprocessing stage aims to smooth the US image and extract the region of interest (ROI). Different color modes (Grayscale, YCBCR, RGB) with Otsu segmentation with different parameters (0.1, 0.17, 0.20) were used in this stage. Additionally, the region property function is applied at the end of this stage to eliminate the surrounding parts of the image containing the patient's personal information. The second stage, which is processing, comprises a variety of enhancement and denoising filters such as the Histogram filter, wiener filter, clahe filter, Gaussian filter, and anisotropic diffusion filter. Finally, in the edge detection stage, four edge detectors are applied, namely: Sobel, Canny, Prewitt, and Roberts with a thresholding value of 0:150.

C. IMAGE PREPROCESSING STAGE

The main objective of the preprocessing stage is to extract the region of interest (ROI) that includes the area

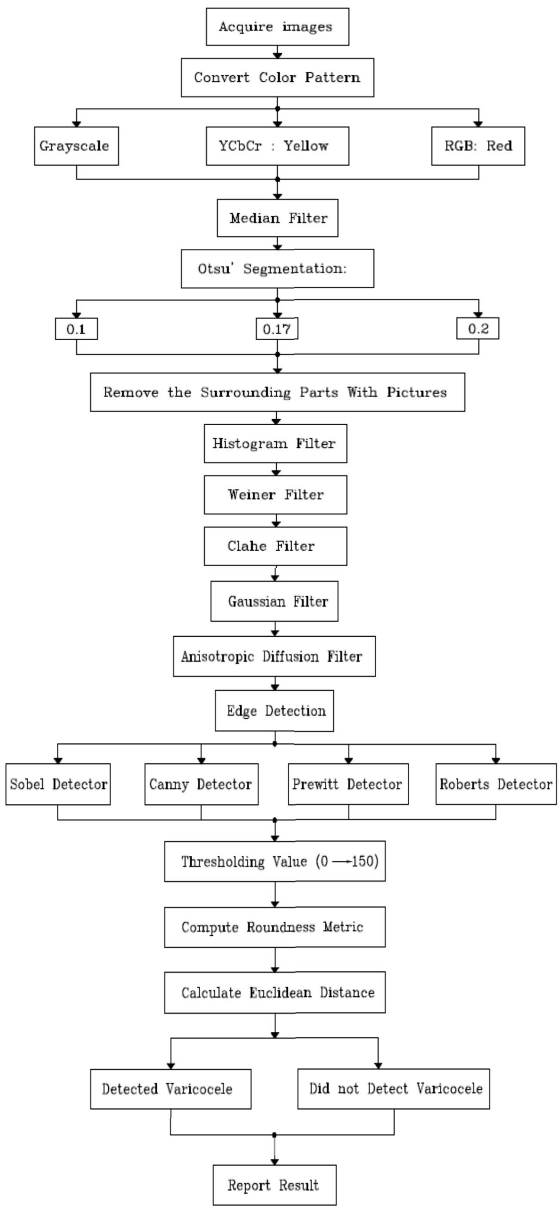

FIGURE 3. **Flowchart for the process of detecting varicocele.**

containing the veins that need to be examined. Common cropping techniques are not suited for this stage because the dataset contains images of varying sizes and dimensions. Furthermore, the veins to be examined appear at different locations in different images.

At the beginning of this stage, different color modes (Grayscale, YCBCR, RGB) are applied followed by applying a median filter. Otsu segmentation is then applied with a set of parameters (0.1, 0.17, 0.20) to remove irrelevant parts such as the writing in the US image.

Determining region property with US images of varying sizes and vein locations is a challenging task. Therefore, Otsu segmentation was used with different parameters to determine the target area. This segmentation technique can move in the high and low areas of the image since these areas have specific values. The applied region property technique is similar to techniques used in the detection of breast cancer [22]. There are a wide variety of image segmentation techniques, each with its advantages and disadvantages. However, we opted to experiment with a stable and fast algorithm like the Otsu segmentation algorithm in contrast to the Watershed algorithm, for example, which is sensitive to noise and prone to over-segmentation [4]. The preprocessing steps are described in detail in the following subsections.

1) COLOR SYSTEMS

Varicocele veins may be scattered over different areas of the testicles. To overcome this problem and increase segmentation efficacy, three different color modes are utilized: Grayscale, YCBCR, and RGB. With RGB, experiments performed using the red, green, and blue channels showed that the red channel was the most accurate. Therefore, it has been chosen for observing the varicocele. Then, the image is converted into YCbCr where the yellow channel is the most significant since YCbCr format stores luminance information as a single component (Y) [23]. Finally, the grayscale mode is used for reducing the complexity of the image as it represents images in two dimensions rather than three dimensions [24]. Additionally, each pixel in the grayscale image is a single sample representing only an amount of light useful for observing a localized region of varicocele. Experiments were conducted using each of these color modes to get the best results for the best color mode. Fig. 4 shows sample results of the preprocessing stage using the YCbCr color mode on one US image of varicocele.

2) MEDIAN FILTER

The median filter helps in setting and smoothing the edges of the input US image so it can be segmented more efficiently. It also helps in reducing impulsive noise or salt-and-pepper noise in the image while preserving the useful features and edges of the image. In this paper, the median filter is used with three color modes. Figure 4-(c) shows an example of using the median filter with the YCbCr color space.

3) OTSU METHOD

The Otsu method was used for image segmentation using different parameters (0.1, 0.17, and 0.2). These three parameters were used with each color mode: grayscale, RGB (red channel), and YCbCr (yellow channel). The use of different parameters aims to get the best segmentation result and find a robust threshold. In this step of Otsu segmentation, the unnecessary parts of the image were removed including the background and the writings on the US image. This keeps only the area in the image containing the possible disease, called the region of interest (ROI), as shown in Fig. 4-(d).

Experimentally, using Otsu segmentation with parameters 0.17 and 0.2 yielded almost the same results. In the next step, the image is transformed into a binary (black and white) image. This conversion helps in determining the desired information about the position and shape of the objects of interest in the image. The advantage of this operation is

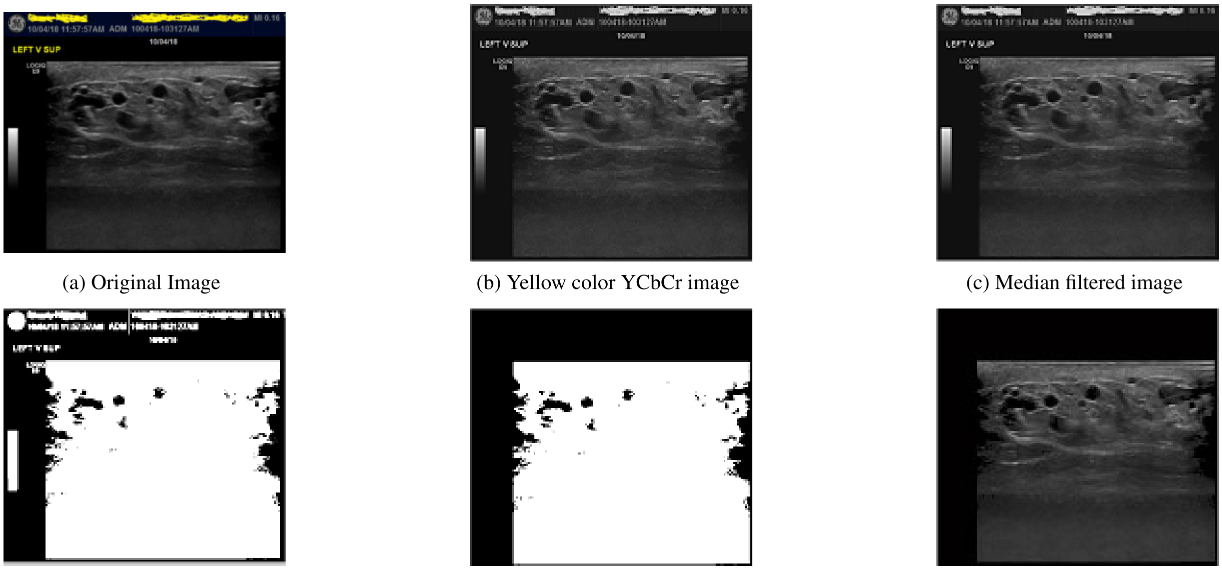

(a) Original Image (b) Yellow color YCbCr image (c) Median filtered image

(d) Otsu (0.1) segmented image (e) Cropped binary image (f) Region Of Interest (ROI)

FIGURE 4. Preprocessing of a sample image.

reducing the data complexity and simplifying the process of recognition as seen in Fig. 4-(e). In the final step of this stage, the technique of region property is used for extracting the ROI by multiplying the image that resulted from the median filter by the image that resulted from the Otsu Segmentation. Figure 5-(f) shows the result of this operation. The image that resulted from the preprocessing stage, which identified and extracted the ROI, is further processed in the next stages.

D. PROCESSING STAGE

The main purpose of this step is to enhance the clarity of the image. The image, in many cases, may contain noise of various kinds. This affects the quality of the information in the picture. In this stage, we remove noise and extract the important information from the image by applying a set of filters. This enhances and smooths the image and prepares it for the next stage, which is edge detection. We studied the impact of each of these filters on the images through a set of experiments to identify the filters that work best with our images. Different arrangements were examined until the best arrangement of these filters was obtained as illustrated in Fig. 6. The result of this stage was an enhanced and smoothed image with the noise removed.

E. EDGE DETECTION

This stage is one of the most important stages for determining the area of the disease. It includes different steps that will be explained in the following subsections. Several edge detection techniques are used including Sobel, Prewitt, Roberts, and Canny where each technique has its characteristics and works independently to identify the most important transients in the image and the disease pathology. These edge detection techniques are described in the following subsection.

1) EDGE DETECTION TECHNIQUES

Different edge-detection techniques have been examined to select the most suitable. First, the Sobel edge detector executes a 2-D spatial gradient computation on the image. It emphasizes regions of high spatial frequency that are equivalent to edges and provides a simple approximation of the gradient magnitude [25]. Second, the Robert edge detector performs a simple and quick computation of the 2-D spatial gradient measurement of the image. It thus highlights regions of high spatial gradient which often correspond to edges [26]. Third, the Prewitt edge detector detects two types of edges; horizontal edges and vertical edges. The edges are computed by using the difference between corresponding pixel strength values [27]. Finally, the Canny edge detector can smooth the image while computing the gradient magnitude and orientation using finite-difference approximations for the partial derivatives and applying non-maxima suppression to the gradient magnitude. It employs the double-thresholding algorithm to detect and link edges [28].

Multiple aspects need to be considered when applying edge detection including the contrast between the objects that need to be segmented and the image background features. Changes in the contrast can be detected by operators that calculate the gradient of the image using a Binary Gradient Mask or a Dilated Gradient Mask. For differentiating the background from the objects of interest, inverse image closing can be applied, and then its result is multiplied by the result of an Anisotropic filter. This will eliminate many unnecessary image details while preserving the region of interest. Figure 7 illustrates this process. Figure 8 shows the result of applying different edge detectors.

2) THRESHOLDING IN EDGE DETECTION

There may be other tissues in the region of interest (ROI) that do not correspond to dilated veins. A group of experiments

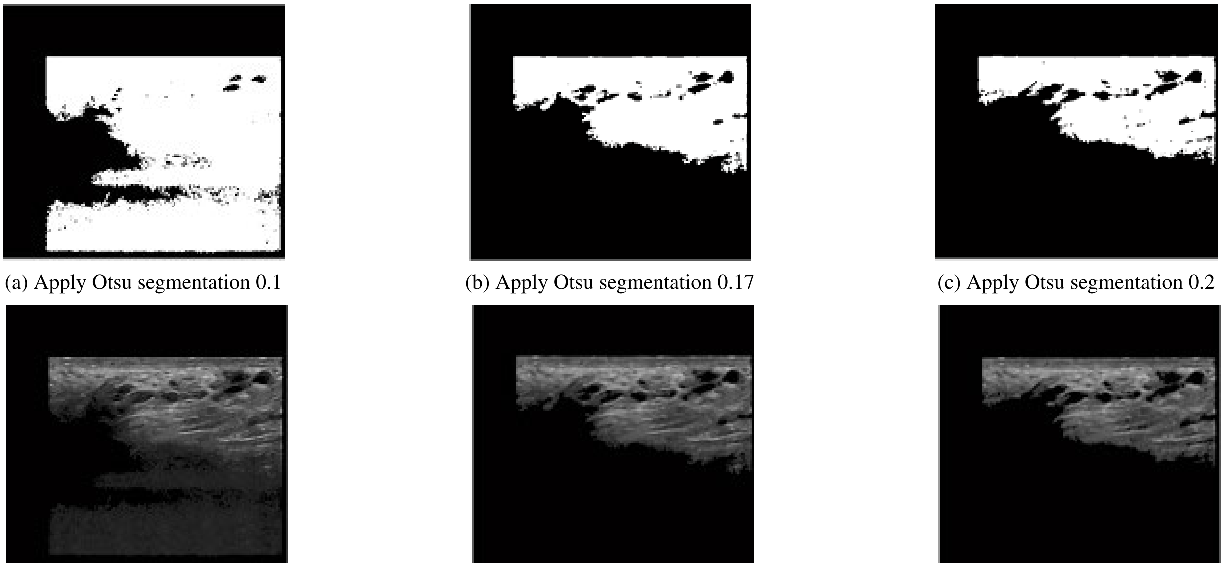

(a) Apply Otsu segmentation 0.1 (b) Apply Otsu segmentation 0.17 (c) Apply Otsu segmentation 0.2

(d) Find ROI for Otsu 0.1 (e) Find ROI for Otsu 0.17 (f) Find ROI for Otsu 0.2

FIGURE 5. **Applying Otsu segmentation with different parameters and finding ROI using the gray color mode.**

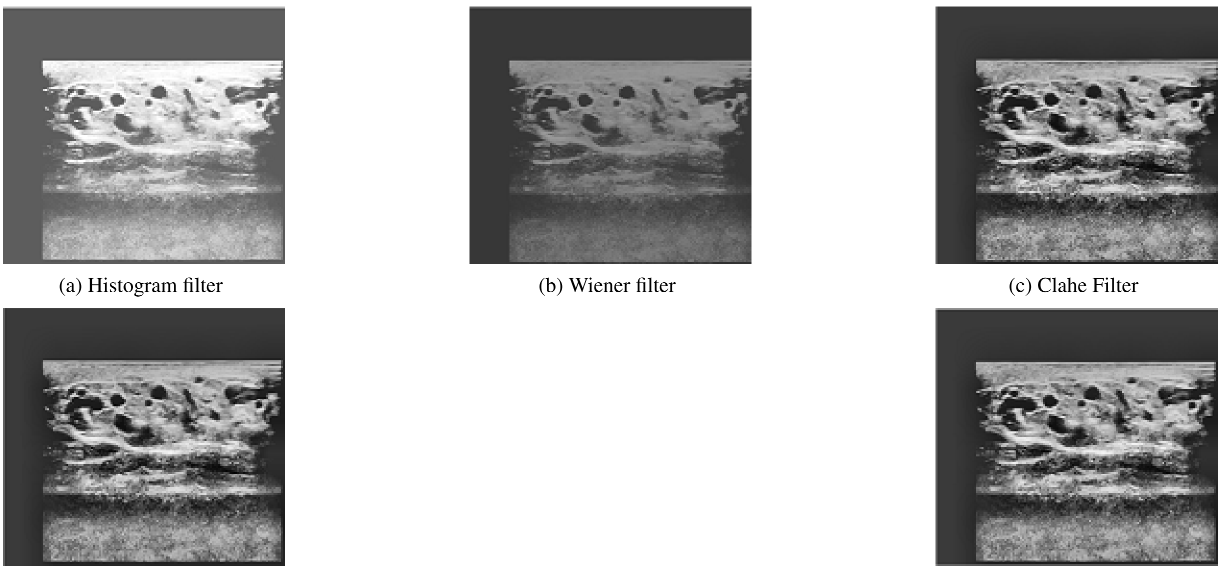

(a) Histogram filter (b) Wiener filter (c) Clahe Filter

(d) Gaussian Filter (e) Anisotropic Diffusion Filter

FIGURE 6. **Applying a filter arrangement in the experiments.**

was done, by applying several thresholding values, to find the appropriate one and eliminate the unnecessary tissues. The best results were achieved with thresholding values between 0-150. This operation is shown in Fig. 7-(F).

3) ROUNDNESS COMPUTATION

In this step, boundaries of the ROI are detected including the outer boundaries of the ROI as well as the boundaries of objects of different shapes that lie inside the ROI. These detected objects inside the ROI may have shapes that vary between circular, semicircular, and other shapes where dilated veins predominantly come in circular and semicircular shapes. The equation of the circle can be used to solve this problem, where the relationship between the circumference of the circle and its area is taken into account. Therefore, a roundness metric is defined for this novel algorithm as in Equation 1 to identify and eliminate non-circular shapes by using a 90-96% circulation ratio. A sample result of this step is shown in Fig. 9-(A), where $metric(k)$ is the roundness percentage of cells.

$$metric(k) = \frac{4 * \pi * area}{2} \tag{1}$$

If the value of $metric(k)$ is equal to 1, this indicates that the object is a circle. Since the infected cells are not perfect circles, we classify the ratio of roundness metric for possibly

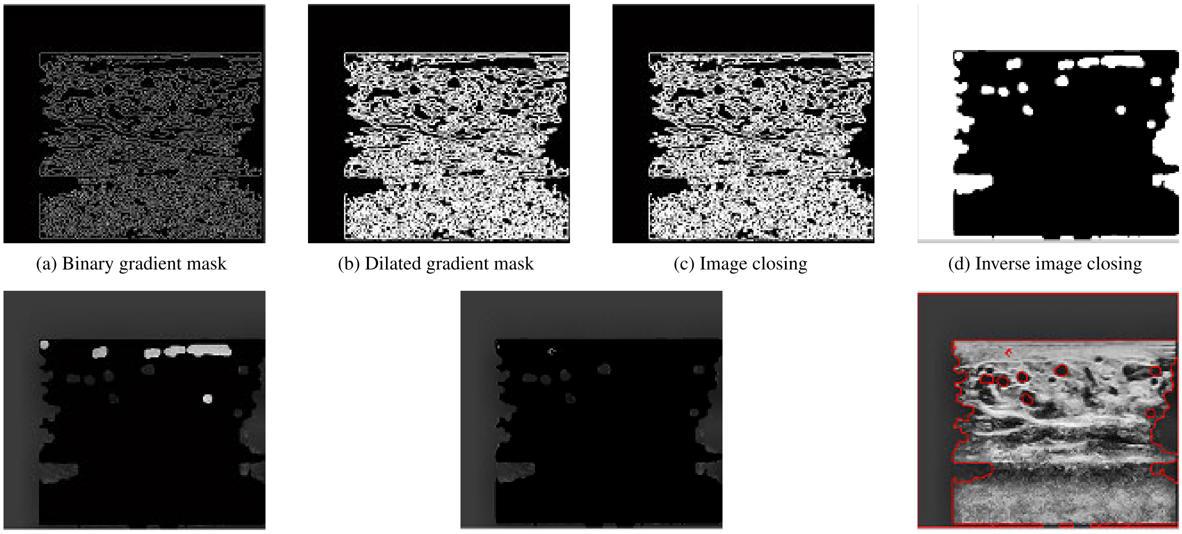

(a) Binary gradient mask (b) Dilated gradient mask (c) Image closing (d) Inverse image closing

(e) Result of multiplying image closing with Anisotropic image (f) Applying thresholding value 0:150 (g) Applying Canny detector to determine the boundaries around dilated veins

FIGURE 7. The operation of detecting dilated veins using the Canny detector, YcbCr color mode, and 0.1 Otsu segmentation.

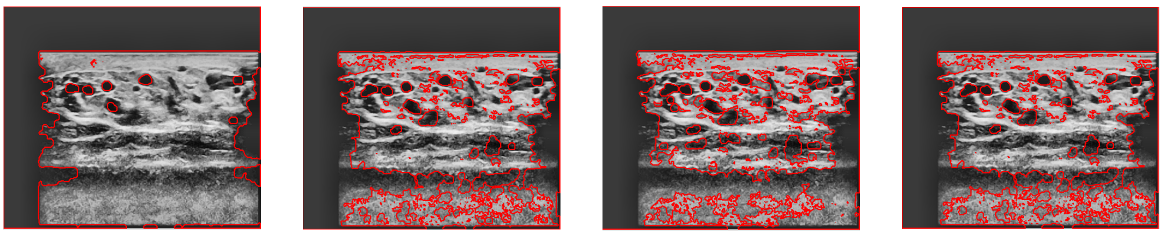

(a) Canny edge detector (b) Prewitt edge detector (c) Robert edge detector (d) Sobel edge detector

FIGURE 8. Results of applying different edge detectors.

dilated veins as follows:

$$metric(k) > 0.9 \;\; and \;\; metric(k) < 0.96$$

4) EUCLIDEAN DISTANCE

Euclidean distance, given by Equation 2, is used for calculating the distance between the edges of marked objects obtained in the previous step to decide if the object is a dilated vein.

$$dist = \sqrt{(x_1 - x_2)^2 + (y_1 - y_2)^2} \tag{2}$$

Furthermore, we limited the distance between two points on the edges of marked objects as follows:

$$dist(i) > 23\, pixel \;\; and \;\; dist(i) < 60\, pixel$$

This range was the most suitable based on empirical results. If the ratio falls outside this range, non-disease-related objects may be falsely identified. Figure 9-(b) shows the Euclidean distances computed for all round shapes in the image. Figure 9-(c) shows the resulting image after eliminating objects with out-of-bounds distances. Figure 9-(d) shows the final detection result of the area that has the disease using the YCbCr color mode. If no dilated objects are detected, the case is identified as normal (with no varicocele). Figure 10 shows the results of detection using gray and red color modes for the same image in Fig. 9.

It should be noted that the procedure developed here is only applicable for detecting enlarged veins in varicocele disease, and was only tested on the given dataset. Other veins in the human body might have different structures or sizes, therefore, there may be a need to adjust the procedure or its parameters if it is going to be used for detecting veins in other parts of the human body.

IV. RESULTS AND DISCUSSION - GRAY COLOR MODE

The system was implemented in MATLAB and applied on a dataset of 90 US images in the DICOM and PNG formats. It was gathered in collaboration with the department of radiology at a local hospital in Amman, Jordan. The images were taken of the left testicles of 90 patients to diagnose varicocele. The dataset consists of 22 normal images and 78 abnormal images as classified by an expert. The images have different sizes because they were taken from various ultrasound machines. The results were evaluated based on the system's ability to detect dilated veins in the abnormal cases and not to detect any veins in the normal cases. The description of the evaluation process is described in the following two subsections.

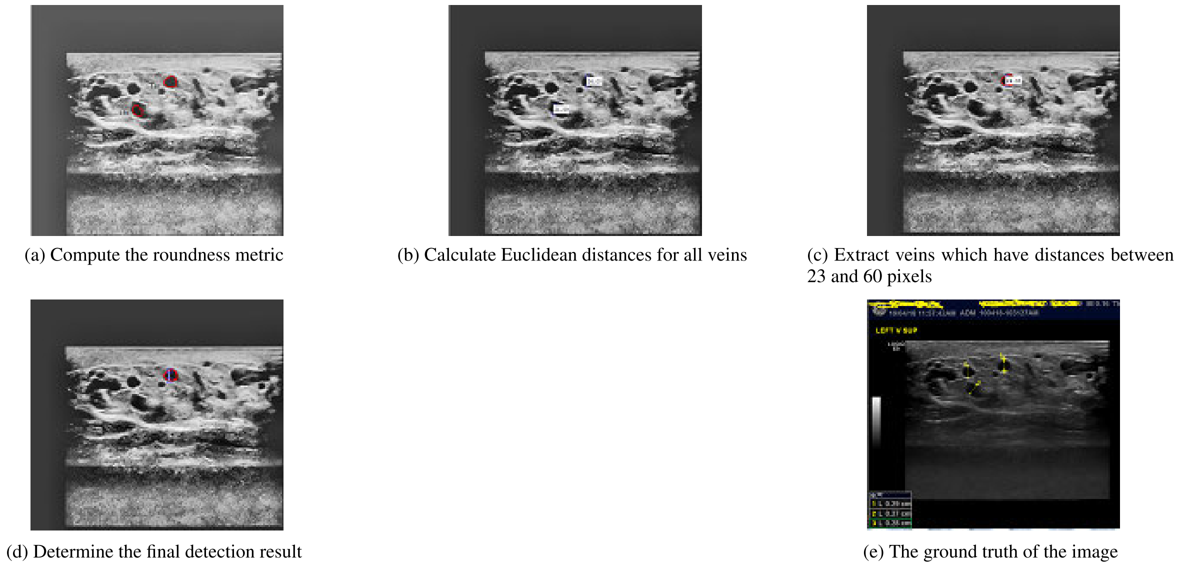

(a) Compute the roundness metric (b) Calculate Euclidean distances for all veins (c) Extract veins which have distances between 23 and 60 pixels (d) Determine the final detection result (e) The ground truth of the image

FIGURE 9. An example of the final detection stage - YCbCr color mode.

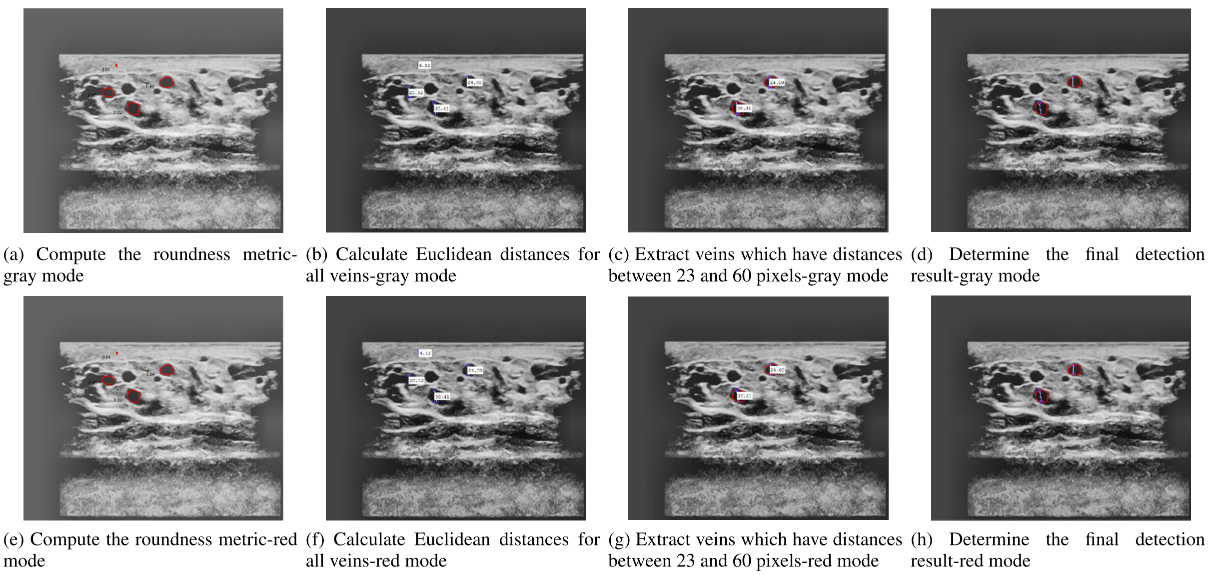

(a) Compute the roundness metric-gray mode (b) Calculate Euclidean distances for all veins-gray mode (c) Extract veins which have distances between 23 and 60 pixels-gray mode (d) Determine the final detection result-gray mode (e) Compute the roundness metric-red mode (f) Calculate Euclidean distances for all veins-red mode (g) Extract veins which have distances between 23 and 60 pixels-red mode (h) Determine the final detection result-red mode

FIGURE 10. An example of the final detection stage - gray and red color modes.

A. CONFUSION MATRIX

The use of a confusion matrix, or a contingency table, is a referencing method used in automated learning to aid the evaluation of the performance of an algorithm. For the proposed algorithm, we used four parameters to represent the relationship between the different ground truths and their classifications: False Negative (FN), True Positive (TP), True Negative (TN), and False Positive (FP). TP is the number of positive cases classified as positive. FP is the number of negative cases classified as positive. TN is the number of negative cases classified as negative. FN is the number of positive cases classified as negative. The accuracy, given in Equation 3, can be defined as the percentage of correctly classified instances [29] where TP, FN, FP, and TN represent the number of true positives, false negatives, false positives, and true negatives, respectively.

$$Accuracy = \frac{TP + TN}{TP + FP + TN + FN} \tag{3}$$

Other standard performance measures can be computed using these parameters as in Equations 4 through 7.

$$Sensitivity = \frac{TP}{TP + FN} \tag{4}$$

$$Specificity = \frac{TN}{TN + FP} \tag{5}$$

$$Positive\ Predictive\ Values(PPV) = \frac{TP}{TP + FP} \tag{6}$$

$$Negative\ Predictive\ Value(NPV) = \frac{TN}{FN + TN} \tag{7}$$

TABLE 1. Confusion matrix.

System Diagnostics	Ground Truth	Measurement
Has varicocele	Has varicocele	TP
Has varicocele	Normal	FP
Normal	Has varicocele	FN
Normal	Normal	TN

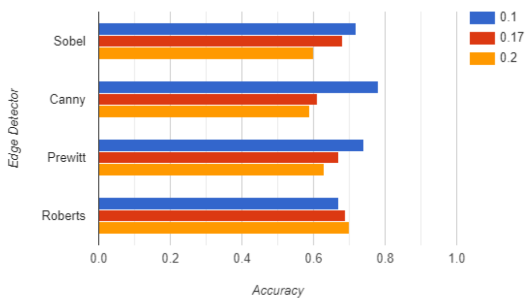

FIGURE 11. Accuracy of Otsu segmentation with different types of edge detection in YCbCr mode.

B. PERFORMANCE MEASUREMENT

The diagnosis of the disease was based on the patient having varicocele indicated by an expanding testicle vein. The ground truth was provided by an expert and used in classifying the system's diagnostics as in Table 1.

C. EDGE DETECTOR PERFORMANCE WITH DIFFERENT PARAMETERS AND COLOR MODES

To determine which edge detector gives the best detection, performance measurements of accuracy, sensitivity, and specificity are used. Figure 11 shows the detection accuracy of using the YCbCr color mode with various edge detectors; namely Soble, Canny, Prewitt, and Roberts. It can be observed that the highest accuracy was achieved using the Canny edge detector with Otsu segmentation of 0.1 using the YCbCr color mode. Similar evaluations were done for the other two color modes; Red and Gray, but the YCbCr mode with the Canny edge detector and 0.1 Otsu segmentation gave the best accuracy.

Similarly, it can be observed from Figure 12 that the highest sensitivity was achieved with 0.1 Otsu using the Canny detector and YCbCr mode. Similar evaluations were done for the red and gray color modes but the mode of YCbCr with the Canny edge detector and 0.1 Otsu segmentation gave the highest sensitivity value.

Likewise, Figure 13 shows that the highest specificity was achieved using the Canny detector with 0.2 Otsu using the YCbCr color mode. However, further evaluations on the red and gray color modes showed that using the Canny detector with 0.2 Otsu achieved the highest specificity in the red color mode.

In Summary, the system showed a Sensitivity of 91% (the test was able to detect 91% of the cases with varicocele) and a Specificity of 39%. Results also showed a Positive Predictive Value (PPV) of 81% (81% of men who tested positive actually have varicocele), and a Negative Predictive

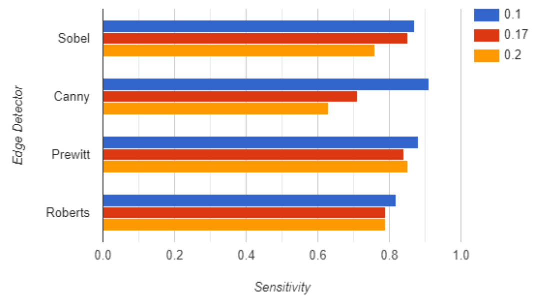

FIGURE 12. Sensitivity of Otsu segmentation with different types of edge detection in YCbCr mode.

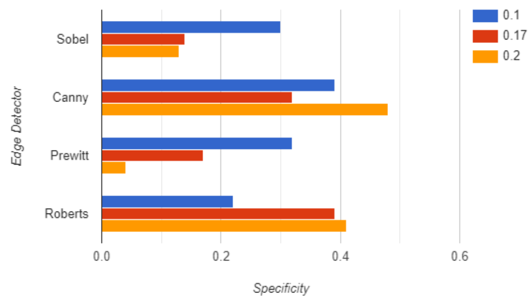

FIGURE 13. Specificity of Otsu segmentation with different types of edge detection in YCbCr mode.

Value (NPV) of 60%. The processing time was a few seconds for a single US image, which is relatively small considering that the implementation was done in MATLAB. Regarding accuracy, it can be concluded that the best edge detector for detecting varicocele is a Canny edge detector with the YCbCr color mode and 0.1 Otsu segmentation as it achieved the highest detection rate of 78%.

V. CONCLUSION AND FUTURE WORK

Varicocele disease can be diagnosed using US images taken of the left and right testicles of a patient in three positions; Supine, Valsalva, and Standing. The supine position was chosen in this research because it is considered by many physicians as the most reliable in diagnosing varicocele. The veins structures in all images are categorized according to two shapes; cross-section and tube structure, where both shapes are detected in the same manner. A novel system has been developed to identify and detect the enlarged veins in US images and to determine whether a patient has varicose veins or not. In this system, images are processed in three stages; preprocessing, processing, and edge detection. In the preprocessing stage, the region of interest (ROI) is extracted from the pampiniform plexus area. In the processing stage, different denoising algorithms, such as the Gaussian filter and the Anisotropic diffusion filter, are used to enhance the image. Finally, in the edge detection stage, four edge detectors are used: Canny, Sobel, Prewitt, and Roberts.

The algorithm was applied to 90 US images that were taken of the left testicles of 90 patients in the supine position. The implementation was tested with three color modes (Gray, RGB, YCbCr), Otsu segmentation with three parameters

(0.1, 0.17, 0.2), and different filtering and edge detection techniques. The results showed that the best accuracy in detecting varicocele was achieved when applying the YCbCr color space yellow (y) channel with 0.1 Otsu segmentation and a Canny edge detector. Currently, we are expanding our work with a new funded project, where we are collecting additional data, and we will be evaluating Deep Learning Convolutional Neural Networks (CNN) for ultrasound image segmentation and classification of the varicocele disease.

REFERENCES

[1] Y. Tang, L. Li, C. Wang, M. Chen, W. Feng, X. Zou, and K. Huang, "Real-time detection of surface deformation and strain in recycled aggregate concrete-filled steel tubular columns via four-ocular vision," *Robot. Comput.-Integr. Manuf.*, vol. 59, pp. 36–46, Oct. 2019.

[2] W. Chenglin, C. Xiong, L. Chunjiang, and T. Yunchao, "Induced pluripotent stem cells recognition and localization," *Acta Microscopica*, vol. 28, no. 5, pp. 1122–1132, 2019.

[3] M. Chen, Y. Tang, X. Zou, Z. Huang, H. Zhou, and S. Chen, "3D global mapping of large-scale unstructured orchard integrating eye-in-hand stereo vision and SLAM," *Comput. Electron. Agricult.*, vol. 187, Aug. 2021, Art. no. 106237.

[4] W. A. Mustafa, N. M. Salleh, S. Z. S. Idrus, M. A. Jamlos, and M. N. K. H. Rohani, "Overview of segmentation X-ray medical images using image processing technique," *J. Phys., Conf.*, vol. 1529, Apr. 2020, Art. no. 042017.

[5] J. Guerrero, S. E. Salcudean, J. A. McEwen, B. A. Masri, and S. Nicolaou, "Real-time vessel segmentation and tracking for ultrasound imaging applications," *IEEE Trans. Med. Imag.*, vol. 26, no. 8, pp. 1079–1090, Aug. 2007.

[6] S. Pauroso, N. Di Leo, I. Fulle, M. Di Segni, S. Alessi, and E. Maggini, "Varicocele: Ultrasonographic assessment in daily clinical practice," *J. Ultrasound*, vol. 14, no. 4, pp. 199–204, Dec. 2011.

[7] S. C. Esteves, C.-L. Cho, A. Majzoub, and A. Agarwal, *Varicocele Male Infertility: A Complete Guide*. Cham, Switzerland: Springer, 2019.

[8] G. Liguori, C. Trombetta, G. Garaffa, S. Bucci, I. Gattuccio, L. Salamè, and E. Belgrano, "Color Doppler ultrasound investigation of varicocele," *World J. Urol.*, vol. 22, no. 5, pp. 378–381, Oct. 2004.

[9] L. Rocher, J.-L. Gennisson, J. Barranger, A. Rachas, A. Criton, V. Izard, M. Bertolloto, M.-F. Bellin, and J.-M. Correas, "Ultrasensitive Doppler as a tool for the diagnosis of testicular ischemia during the valsalva maneuver: A new way to explore varicoceles?" *Acta Radiol.*, vol. 60, no. 8, pp. 1048–1056, 2019.

[10] B. B. Najari, M. J. Katz, M. L. Schulster, D. J. Lee, P. S. Li, and M. Goldstein, "Increased body mass index in men with varicocele is associated with larger spermatic vein diameters when supine," *Urology*, vol. 89, pp. 40–44, Mar. 2016.

[11] D. Angelova and L. Mihaylova, "Contour segmentation in 2D ultrasound medical images with particle filtering," *Mach. Vis. Appl.*, vol. 22, pp. 551–561, Apr. 2010.

[12] R. C. Gonzalez, R. E. Woods, and B. R. Masters, *Digital Image Processing*, 3rd ed. London, U.K.: Pearson, 2008.

[13] D. L. Pham, C. Xu, and J. L. Prince, "Current methods in medical image segmentation," *Annu. Rev. Biomed. Eng., Annu. Rev.*, vol. 2, no. 1, pp. 315–337, 2000.

[14] M. A. A. Rahim, N. Othman, and W. M. H. W. Mahmud, "Preliminary study of image processing techniques for the detection of varicocele based on 2D ultrasound images," *J. Phys., Conf.*, vol. 1049, Jul. 2018, Art. no. 012074.

[15] E. Karami, M. S. Shehata, and A. Smith, "Tracking of the internal jugular vein in ultrasound images using optical flow," in *Proc. IEEE 30th Can. Conf. Electr. Comput. Eng. (CCECE)*, Apr. 2017, pp. 1–4.

[16] M. S. Ahmed and B. Indira, "Morphological technique for detection of microaneurysms from RGB fundus images," in *Proc. Int. Conf. Wireless Commun., Signal Process. Netw. (WiSPNET)*, Mar. 2017, pp. 44–47.

[17] M. Ikhsan, K. K. Tan, A. S. Putra, T. H. S. Chew, and C. F. Kong, "Automatic identification of blood vessel cross-section for central venous catheter placement using a cascading classifier," in *Proc. 39th Annu. Int. Conf. IEEE Eng. Med. Biol. Soc. (EMBC)*, Jul. 2017, pp. 1489–1492.

[18] J. Kang, Z. Ma, H. Li, L. Xu, and L. Zhang, "Automatic detection of arteriovenous nicking in retinal images," in *Proc. IEEE 11th Conf. Ind. Electron. Appl. (ICIEA)*, Jun. 2016, pp. 795–800.

[19] L. Licev, K. Feberova, J. Tomecek, and J. Hendrych, "An enhanced method for automatic detection and segmentation of carotid artery in ultrasound images," in *Proc. 17th Int. Conf. Comput. Syst. Technol.*, Jun. 2016, pp. 206–213.

[20] F. Ghadiri, M.-R. Akbarzadeh-T, and S. Haddadan, "Vessel segmentation based on Sobel operator and fuzzy reasoning," in *Proc. 1st Int. eConf. Comput. Knowl. Eng. (ICCKE)*, Oct. 2011, pp. 189–194.

[21] B. Sciolla, L. Cowell, T. Dambry, B. Guibert, and P. Delachartre, "Segmentation of skin tumors in high-frequency 3-D ultrasound images," *Ultrasound Med. Biol.*, vol. 43, no. 1, pp. 227–238, Jan. 2017.

[22] A. Martellosio, M. Pasian, M. Bozzi, L. Perregrini, A. Mazzanti, F. Svelto, P. E. Summers, G. Renne, L. Preda, and M. Bellomi, "Dielectric properties characterization from 0.5 to 50 GHz of breast cancer tissues," *IEEE Trans. Microw. Theory Techn.*, vol. 65, no. 3, pp. 998–1011, Dec. 2016.

[23] E. Prathibha, S. Yellampalli, A. Manjunath, and Y. Bangalore, "Design and implementation of color conversion module RGB to YCbCr and vice versa," *Int. J. Comput. Sci. Issues*, vol. 1, no. 1, 2011.

[24] T. Kumar and K. Verma, "A theory based on conversion of RGB image to gray image," *Int. J. Comput. Appl.*, vol. 7, no. 2, pp. 7–10, Sep. 2010.

[25] C. I. Gonzalez, P. Melin, J. R. Castro, O. Mendoza, and O. Castillo, "An improved Sobel edge detection method based on generalized type-2 fuzzy logic," *Soft Comput.*, vol. 20, no. 2, pp. 773–784, Feb. 2016.

[26] G. Shrivakshan and C. Chandrasekar, "A comparison of various edge detection techniques used in image processing," *Int. J. Comput. Sci. Issues*, vol. 9, no. 5, p. 269, Sep. 2012.

[27] T. Sahoo and S. Pine, "Design and simulation of various edge detection techniques using MATLAB simulink," in *Proc. Int. Conf. Signal Process., Commun., Power Embedded Syst. (SCOPES)*, Oct. 2016, pp. 1224–1228.

[28] R. Kirti and A. Bhatnagar, "Image segmentation using Canny edge detection technique," *Proc. Int. J. Techno-Manage. Res.*, vol. 4, no. 4, pp. 8–14, 2017.

[29] S. Aruna, S. Rajagopalan, and L. Nandakishore, "Knowledge based analysis of various statistical tools in detecting breast cancer," *Comput. Sci. Inf. Technol.*, vol. 2, pp. 37–45, Jul. 2011.

OMAR ALZOUBI received the Ph.D. degree from the School of Electrical and Information Engineering, The University of Sydney, Australia, in 2012. He is currently an Assistance Professor with the Department of Computer Science, Jordan University of Science and Technology, Jordan. His research interests include intelligent systems and machine learning.

MOHAMMAD ABU AWAD received the master's degree in computer science from Jordan University of Science and Technology (JUST), Jordan, in 2019. His research interests include machine learning and signal processing.

AYMAN M. ABDALLA received the Ph.D. degree from the University of Central Florida, Orlando, FL, USA, in 2001. He is currently an Associate Professor of computer science with the Al-Zaytoonah University of Jordan. His research interest includes image and video processing.